

VIBRATION ANALYSIS AND VIBROACOUSTICS

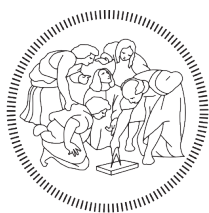
FIRST ASSIGNMENT

Report

Axial vibration of undamped and damped bars

Students

Marco BERNASCONI - 10669941
Alberto DOIMO - 10865196



POLITECNICO
MILANO 1863

Contents

1	Natural Frequencies and Mode Shapes	2
1.1	Vibration of Free-Fixed bar	2
1.2	Vibration of Free-Free bar	3
2	FRF of Axial Vibrations (Free-Fixed Bar)	5
2.1	Undamped free-fixed bar	5
2.2	Damped free-fixed bar (wave propagation equation)	7
2.3	Damped free-fixed bar (modal superposition)	7
3	Driving-point impedance (Free-Fixed damped Bar)	11
3.1	Damped bar (Wave Propagation Solution) with given structural loss factor . . .	11
3.2	Damped bar (Modal Superposition Approach) with given structural loss factor .	11

Chapter 1

Natural Frequencies and Mode Shapes

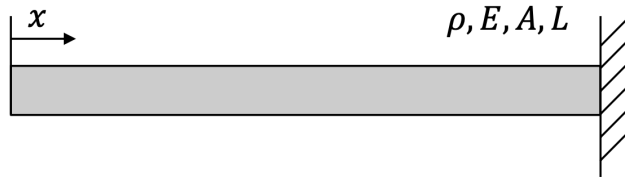


Figure 1.1: Bar free-fixed configuration

The aim is to analyze a bar with the following characteristics: $L = 2 \text{ m}$ $\rho = 2700 \text{ kg/m}^3$ Density $b = 0.05 \text{ m}$ $E = 70 \text{ GPa}$ Young's Modulus $h = 0.05 \text{ m}$

The studies are going to be performed in the frequency range $[0 - 10000] \text{ Hz}$

The axial vibration of a bar are given by the one-dimensional wave equation

$$\frac{\partial^2 u}{\partial x^2} = \frac{1}{c^2} \frac{\partial^2 u}{\partial t^2} \quad (1.1)$$

where $c = \sqrt{\rho/E} = 5092[\text{m/s}]$ is the wave velocity in the bar. In order to find the natural frequencies of the system and the corresponding modeshapes we need to impose standing-wave solution of the one-dimensional wave equation as

$$u(x, t) = \Omega(x) \cdot G(t) = (A \sin(kx) + B \cos(kx)) e^{i\omega t} \quad (1.2)$$

where $k = \omega/c = \omega\sqrt{E/\rho}$.

1.1 Vibration of Free-Fixed bar

In order to find the solution for the Free-fixed configuration we need to set appropriate conditions boundary conditions

$$\begin{cases} N(0, t) = E \cdot bh \cdot \frac{\partial u}{\partial x} \Big|_{x=0} \equiv E \cdot bh \cdot \frac{\partial \Phi}{\partial x} \Big|_{x=0} \cdot e^{i\omega t} = 0 \\ u(L, t) = 0 \end{cases} \quad (1.3)$$

from this system we obtain that

$$\begin{cases} A = 0 \\ B \cos(kL) = 0 \end{cases} \quad (1.4)$$

from the second equation we can assume the harmonic wave solution as

$$k_i = \frac{2\pi}{\lambda_i} = \frac{(2i-1)\pi}{2L} \quad i = 1, 2, \dots, \infty \quad (1.5)$$

from the wave-number we can extrapolate the natural frequency for all the solutions as

$$f_i = \frac{\omega_i}{2\pi} = \frac{k_i c}{2\pi} = \frac{(2i-1)}{4L} \sqrt{\frac{E}{\rho}} \quad (1.6)$$

the i^{th} modeshape therefore becomes

$$\Omega_i(x) = \cos(k_i x) = \cos\left(\frac{(2i-1)\pi}{2L}x\right) \quad (1.7)$$

In figure 1.2 the modeshapes $\Omega_i(x)$ in range $[0, 10000]$ Hz are presented.

Free-Fixed bar resonances and modeshapes

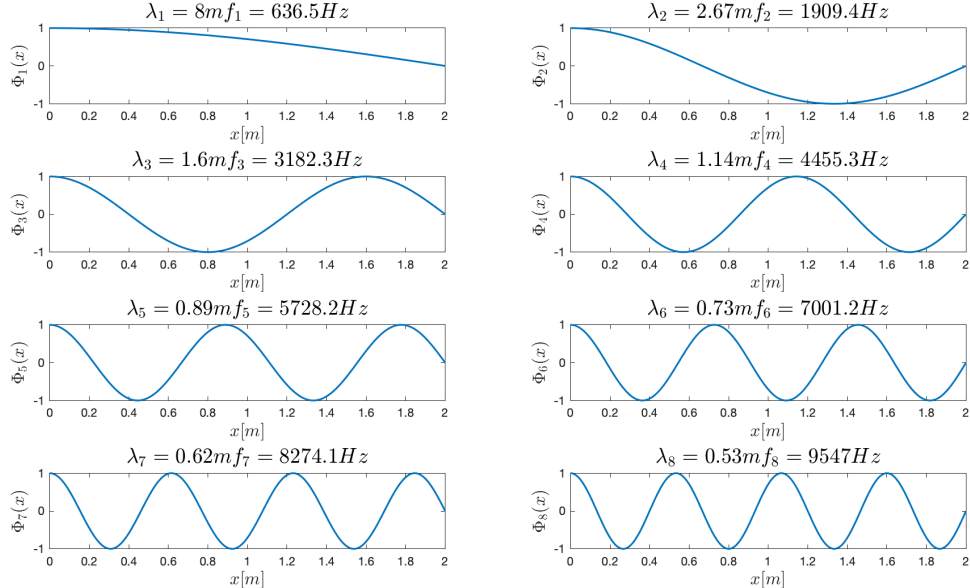


Figure 1.2: Bar free-fixed harmonic wave solution

1.2 Vibration of Free-Free bar

For the calculation of the natural frequencies for the Free-Free configuration the boundary conditions applied are:

$$\begin{cases} N(0, t) = E \cdot bh \cdot \frac{\partial u}{\partial x} \Big|_{x=0} \equiv E \cdot bh \cdot \frac{\partial \Phi}{\partial x} \Big|_{x=0} \cdot e^{i\omega t} = 0 \\ N(L, t) = E \cdot bh \cdot \frac{\partial u}{\partial x} \Big|_{x=L} \equiv E \cdot bh \cdot \frac{\partial \Phi}{\partial x} \Big|_{x=L} \cdot e^{i\omega t} = 0 \end{cases} \quad (1.8)$$

from this we obtain

$$\begin{cases} A = 0 \\ B \sin(kL) = 0 \end{cases} \quad (1.9)$$

from the second equation we can assume the harmonic wave solution as

$$k_i = \frac{2\pi}{\lambda_i} = \frac{i\pi}{L} \quad i = 1, 2, \dots, \infty \quad (1.10)$$

from the wave-number we can extrapolate the natural frequency for all the solutions as

$$f_i = \frac{\omega_i}{2\pi} = \frac{k_i c}{2\pi} = \frac{i}{2L} \sqrt{\frac{E}{\rho}} \quad (1.11)$$

the i^{th} modeshape therefore becomes

$$\Omega_i(x) = \cos(k_i x) = \cos\left(\frac{i\pi}{L}x\right) \quad (1.12)$$

In figure 1.3 the modeshapes $\Omega_i(x)$ in range [0, 10000] Hz are presented.

Free-Free bar resonances and modeshapes

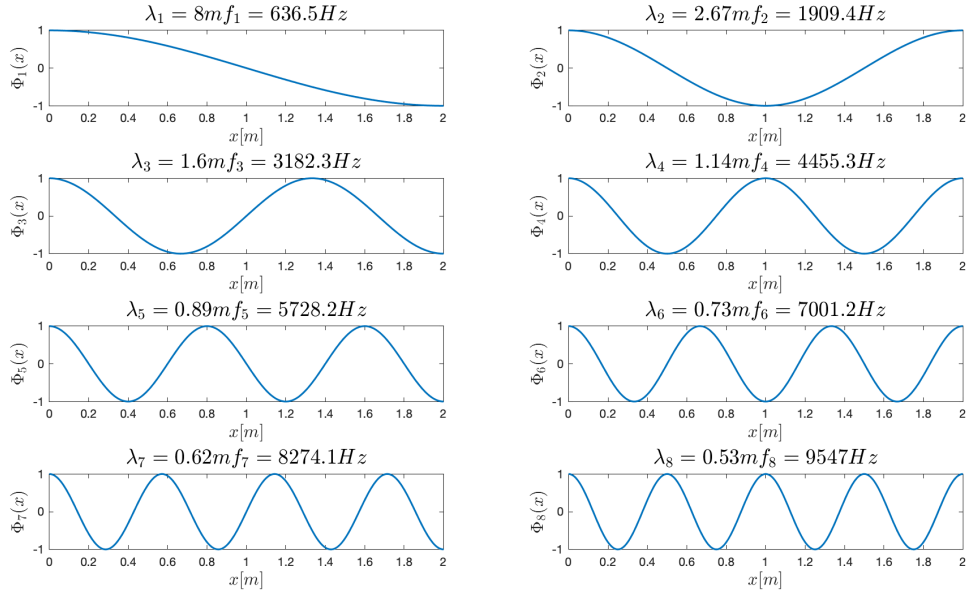


Figure 1.3: Bar free-free harmonic wave solution

Chapter 2

FRF of Axial Vibrations (Free-Fixed Bar)

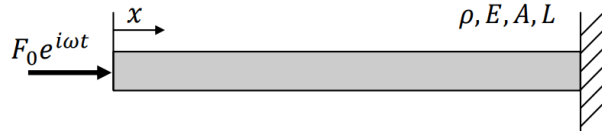


Figure 2.1: Complete view of the system under study

Here in this section we want to study the Frequency Response Function of the free-fixed bar, excited at the free end, taking as output two coordinates \bar{x} . We aim to observe and compare three different approaches to determine the FRF:

- Undamped bar (using the standing wave solution)
- Damped bar (using the wave propagation solution), assuming the loss factor $\eta = 0.01$
- Damped bar (using the modal superposition approach), assuming the loss factor $\eta = 0.01$

We also assume the excitement is given by an harmonic force $F(t) = F_0 e^{i\omega t}$ applied as shown in figure 2.1

2.1 Undamped free-fixed bar

In this section we aim to exploit the standing wave solution of the cantilever bar, allowed by the undamped condition of the bar. We start from the formulation of the standing wave solution of the axial displacement given by:

$$u(x, t) = [A \sin(kx) + B \cos(kx)] e^{i\omega t} \quad (2.1)$$

Now we impose the boundary conditions of the bar in order to retrieve the coefficients A, B :

$$\begin{cases} Ebh \frac{\partial u}{\partial x} \Big|_{x=0} + F_0 e^{i\omega t} = 0 \\ u(L, t) = 0 \end{cases} \quad (2.2)$$

The first boundary condition derives from the force equilibrium, recalling that the reactive force of the bar is $N = bhE\varepsilon_x = bhE\partial u/\partial x$ from the Hooke's law, while the second one simply

describes the fixed right side of the bar. From the first condition we can retrieve the coefficient A since:

$$bhEAke^{i\omega t} + F_0e^{i\omega t} = 0 \longrightarrow A = -\frac{F_0}{bhEk} \quad (2.3)$$

Subsequently putting the found coefficient A in the wave equation we can retrieve the second coefficient thanks to the second boundary condition as:

$$[A \sin(kL) + B \cos(kL)] = 0 \longrightarrow B = \frac{F_0 \sin(kL)}{bhEk \cos(kL)} \quad (2.4)$$

After the application of the trigonometric properties we obtain the following expression of the wave equation:

$$u(x, t) = \frac{F_0 \sin(k(L-x))}{bhEk \cos(kL)} e^{i\omega t} \quad (2.5)$$

now if we fix a generic coordinate $x = \bar{x}$ we can compute the FRF in that decided point of the bar as:

$$H_{und}(\omega) = \frac{u(\bar{x}, \omega)}{F(\omega)} = \frac{F_0 \sin(k(L-\bar{x}))}{bhEk \cos(kL)} e^{i\omega t} \frac{1}{F_0 e^{i\omega t}} = \frac{\sin(k(L-\bar{x}))}{bhEk \cos(kL)} \quad (2.6)$$

$$H_{und}(\omega) = \frac{\sin(k(L-\bar{x}))}{bhEk \cos(kL)} \quad (2.7)$$

Hence, we can iterate the computation of the FRF over the frequency axis recalling that $k = \omega/c = \omega\sqrt{\rho/E}$ and plot it considering two different coordinates $\bar{x}_1 = L/2$ and $\bar{x}_2 = L/5$, the results are visible in figure 2.2.

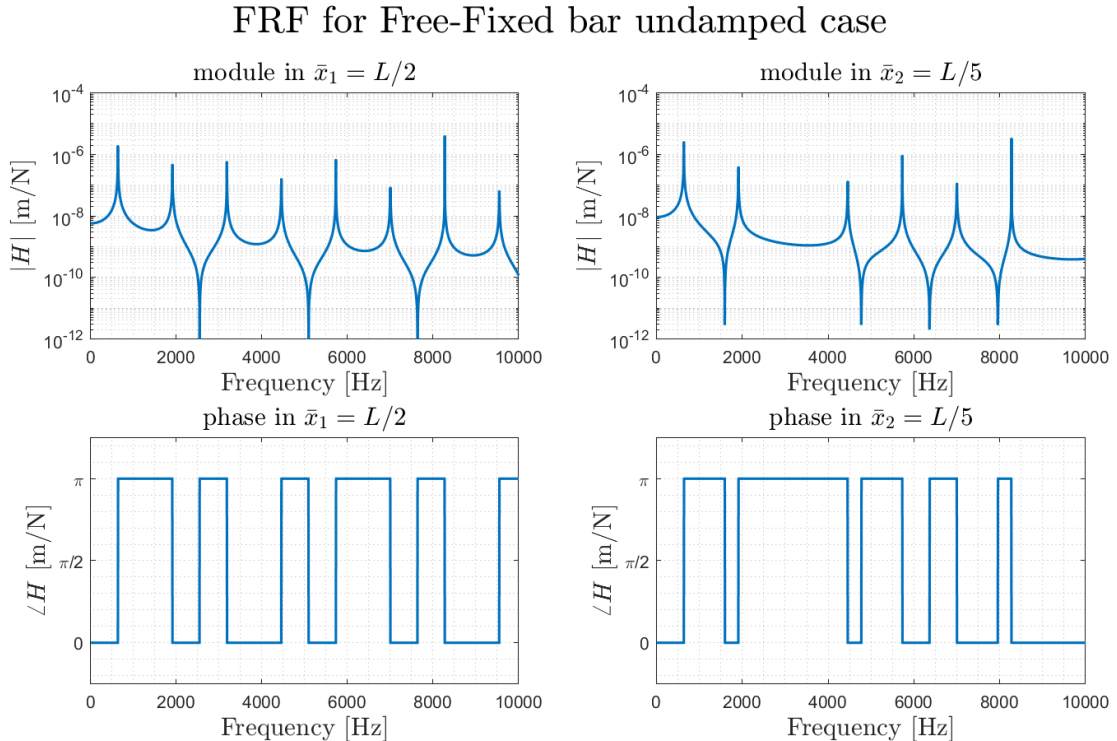


Figure 2.2: FRF for the cantilever bar undamped

2.2 Damped free-fixed bar (wave propagation equation)

Here the cantilever bar is considered no more undamped but viscoelastic effects of the material are taken into account. The viscoelasticity of the bar can be described by the loss factor η which describes how much is the damping force F_{vis} with respect to the elastic force F_{el} .

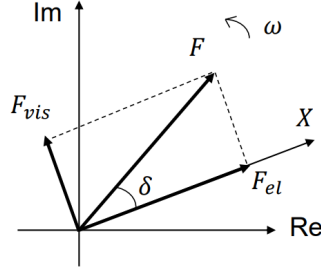


Figure 2.3: Viscoelastic force balance

The loss factor can also be defined as $\eta = \tan(\delta)$, where δ is the phase difference between the total force F and the elastic force F_{el} . Small values of η tell us that the system is lightly damped, while for big values the damping force tends to dominate over the elastic force. Considering the loss factor we introduce the complex Young Modulus $E' = E(1 + i\eta)$ which allows us to write the wave equation:

$$E(1 + i\eta) \frac{\partial^2 u}{\partial x^2} = \rho \frac{\partial^2 u}{\partial t^2} \quad (2.8)$$

From which we can retrieve the new axial wave velocity $c' = \sqrt{E'/\rho}$ and the wavenumber $k' = k(1 + i\eta/2)$. The guessed solution therefore becomes:

$$u(x, t) = A_1 e^{i(\omega t - k'x)} + A_2 e^{i(\omega t + k'x)} \quad (2.9)$$

Being the wavenumber complex, a spacial damping, due to evanescent waves, will appear. The boundary conditions are the same applied in the previous section, hence the solution of the displacement, written in phasorial form is:

$$u(x, t) = \frac{F_0(e^{ik'(L-x)} - e^{-ik'(L-x)})}{ibhk'E'(e^{ik'L} + e^{-ik'L})} e^{i\omega t} \quad (2.10)$$

The Frequency Response Function for a fixed coordinate \bar{x} becomes:

$$H(\omega) = \frac{(e^{ik'(L-\bar{x})} - e^{-ik'(L-\bar{x})})}{ibhk'E'(e^{ik'L} + e^{-ik'L})} \quad (2.11)$$

If we iterate the computation of the FRF over the desired frequency range we obtain the results visible in figure 2.4.

2.3 Damped free-fixed bar (modal superposition)

The effects due to viscoelasticity properties of the material on the FRF can also be retrieved through the use of the modal superposition approach, where every modal parameter is computed starting from the given ones. As first thing we can express the displacement as sum of all the eigenmodes multiplied by the modal coordinate functions:

$$u(x, t) \approx \sum_i \Phi_i(x) q_i(t) = \underline{\Phi}^T(x) \underline{q}(t) \quad (2.12)$$

FRF for Free-Fixed bar damped case $\eta = 0.01$ wave propagation equation

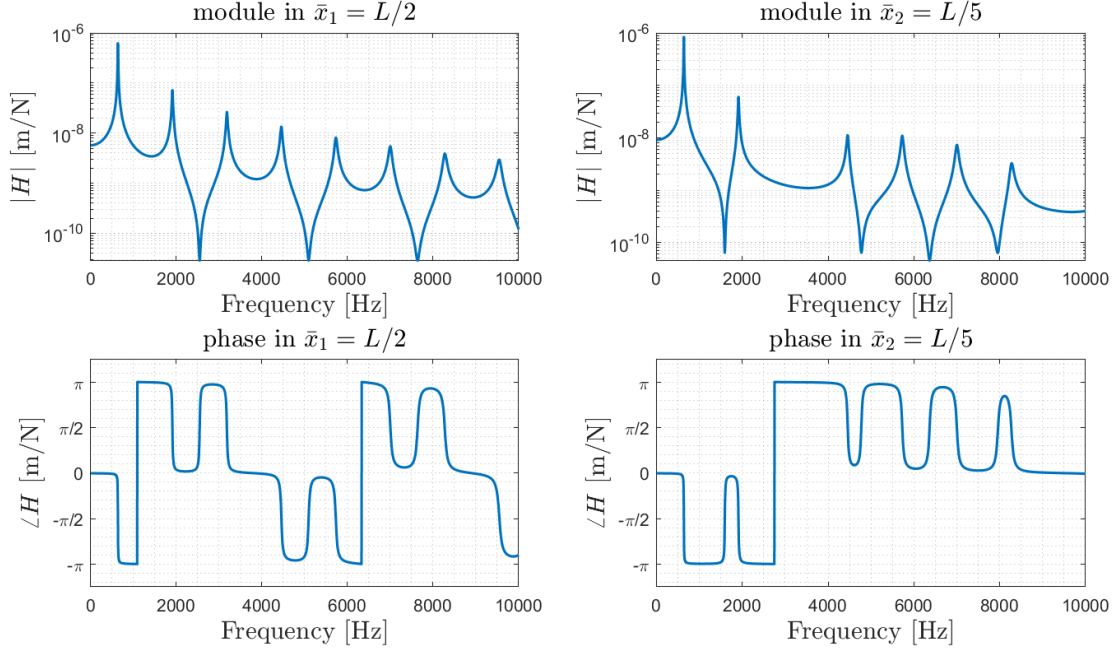


Figure 2.4: FRF for a cantilever bar damped - $\eta = 0.01$

In order to compute the displacement $u(x, t)$ we first need to compute the time evolution of the modal independent coordinates $q_i(t)$. An efficient way to do this is exploiting the Euler-Lagrange equation:

$$\left\{ \frac{d}{dt} \left(\frac{\partial T}{\partial \dot{q}} \right) \right\}^T - \left\{ \frac{\partial T}{\partial q} \right\}^T + \left\{ \frac{\partial D}{\partial \dot{q}} \right\}^T + \left\{ \frac{\partial V}{\partial q} \right\}^T = \underline{Q}_q \quad (2.13)$$

where $\underline{Q}_q = \Phi(0)F_0e^{i\omega t}$. We can now compute all the members of the equation starting from the kinetic energy T :

$$T = \frac{1}{2}m \int_0^L \left(\frac{\partial u}{\partial t} \right)^T \left(\frac{\partial u}{\partial t} \right) dx = \frac{1}{2}\dot{\underline{q}}(t)^T [\underline{M}] \dot{\underline{q}}(t) \quad (2.14)$$

where $\frac{\partial u}{\partial t} = \Phi(t)^T \dot{\underline{q}}(t)$ and $[\underline{M}]$ is the $N \times N$ modal mass matrix where the element (r, s) is computed:

$$m_{r,s} = \int_0^L m \cos(k_r x) \cos(k_s x) dx \quad (2.15)$$

Now we write down the expressio of the elastic potential energy:

$$V_{el} = \frac{1}{2}bhE \int_0^L \left(\frac{\partial u}{\partial x} \right)^T \left(\frac{\partial u}{\partial x} \right) dx = \frac{1}{2}\dot{\underline{q}}(t)^T [\underline{K}] \dot{\underline{q}}(t) \quad (2.16)$$

where $\frac{\partial u}{\partial x} = \Phi'(t)^T \dot{\underline{q}}(t)$ and $[\underline{K}]$ is the $N \times N$ modal stiffness matrix where the element (r, s) can be computed as:

$$k_{r,s} = \int_0^L bhEk_r k_s \sin(k_r x) \sin(k_s x) dx \quad (2.17)$$

Since the modal superposition tells us that the equations of the system are independent, and therefore the matrices $[M]$, $[K]$ are diagonal, so it is enough to compute elements that lie on the diagonal.

$$\begin{cases} m_i = \int_0^L m \cos^2 \left(\frac{(2i-1)\pi}{2L} x \right) \\ k_i = \int_0^L b h E \left(\frac{(2i-1)\pi}{2L} \right)^2 \sin \left(\frac{(2i-1)\pi}{2L} x \right) \end{cases} \quad (2.18)$$

where $\frac{(2i-1)\pi}{2L}$ is the wavenumber of the i -th mode. So now the i -th equation of the decoupled system is:

$$m_i \ddot{q}_i + (1 + j\eta)k_i q_i = \Phi_i(0)F_0 e^{j\omega t} \quad \text{for } i = 1, 2, \dots, N \quad (2.19)$$

using as j as imaginary unit for notation comfort. Setting $q_i(t) = q_{0,i} e^{j\omega t}$ we can rewrite the i -th equation of motion in the form:

$$(-\omega^2 m_i + (1 + j\eta)k_i)q_{0,i} = \Phi_i|_{\bar{x}_{force}} F_0 \quad (2.20)$$

which leads to the expression of the modal coordinate:

$$q_{0,i} = \frac{\Phi_i|_{\bar{x}_{force}} F_0}{-\omega^2 m_i + (1 + j\eta)k_i} \quad (2.21)$$

where \bar{x}_{force} is the coordinate where the force is applied.

If we want to retrieve the response in a generic coordinate different from the driving one we can apply the standard modal superposition formula:

$$u(\bar{x}_{resp}, t) = \sum_{i=1}^N \Phi_i|_{\bar{x}_{resp}} \frac{\Phi_i|_{\bar{x}_{force}} F_0}{-\omega^2 m_i + (1 + j\eta)k_i} \quad (2.22)$$

and from this equation we can compute the FRF simply dividing the displacement by the driving force:

$$H(\omega) = \frac{u(\bar{x}_{resp}, \omega)}{F_0(\omega)} = \sum_{i=1}^N \frac{\Phi_i|_{\bar{x}_{resp}} \Phi_i|_{\bar{x}_{force}}}{-\omega^2 m_i + (1 + j\eta)k_i} = \sum_{i=1}^N \frac{\cos \left(\frac{(2i-1)\pi}{2L} \bar{x}_{resp} \right)}{-\omega^2 m_i + (1 + j\eta)k_i} \quad (2.23)$$

with the formula above we're able to compute the FRF of the system up to 8 modes, for which we have computed the modeshape in section 1. The results are visible in figure ?? and we can clearly see that for the 8 modes considered the response is accurately approximated.

FRF for Free-Fixed bar damped case $\eta = 0.01$
modal superposition approach

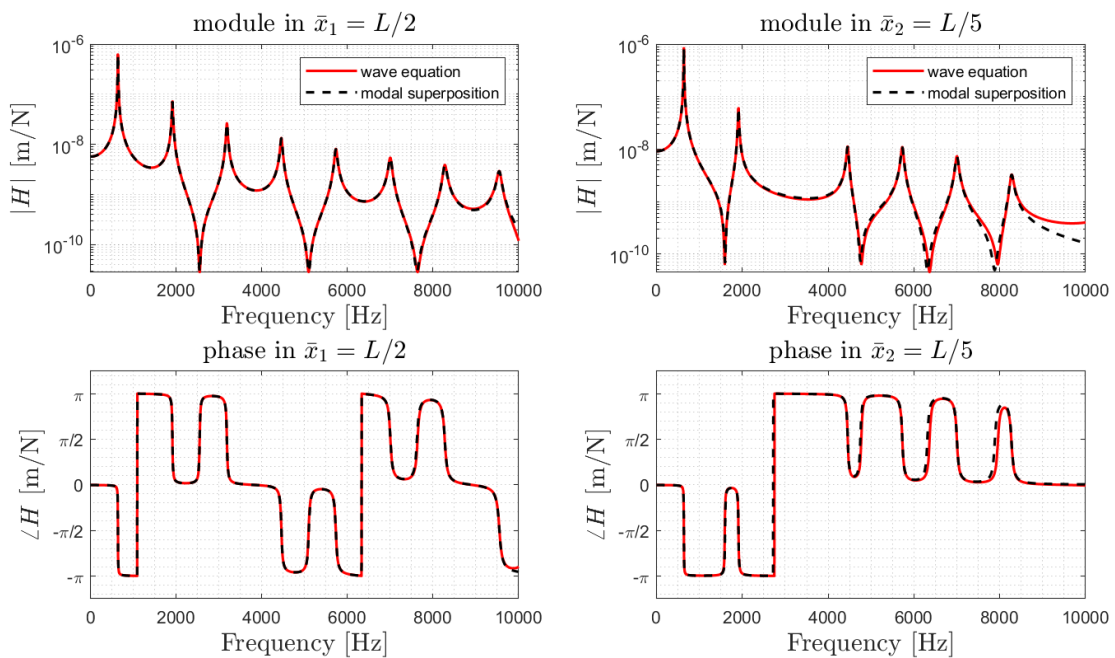


Figure 2.5: FRF for a cantilever bar damped - $\eta = 0.01$ modal superposition approach compared to the one obtained with the wave equation

Chapter 3

Driving-point impedance (Free-Fixed damped Bar)

In this section we want to compute the study of the driving-point impedance in the free end for the damped bar in free-fixed configuration assuming loss factor $\eta = 0.01$ exploiting both the wave propagation solution approach and the modal superposition approach. Assuming a driving force defined by the equation

$$F(t) = F_0 e^{j\omega t} \quad (3.1)$$

the force is applied in $x = 0$, therefore the driving-point impedance can be computed as

$$Z(\omega) = \frac{F(t)}{v(0, t)} = \frac{F_0 e^{j\omega t}}{\left. \frac{\partial u}{\partial t}(x, t) \right|_{x=0}} \quad (3.2)$$

3.1 Damped bar (Wave Propagation Solution) with given structural loss factor

In order to compute the driving point impedance through the propagation solution we need to compute the time-derivation of $u(x, t)$ found in equation 2.10

$$Z(\omega) = \frac{F(t)}{v(0, t)} = \frac{F_0 e^{j\omega t}}{\left. \frac{\partial u}{\partial t}(x, t) \right|_{x=0}} \equiv \frac{k' E' b h (e^{ik'L} + e^{-ik'L})}{(e^{ik'L} - e^{-ik'L}) \omega} \quad (3.3)$$

The solution to this calculation is shown in figure 3.1

3.2 Damped bar (Modal Superposition Approach) with given structural loss factor

In order to calculate the driving point impedance we apply the equation 3.2, using as definition for the displacement $u(x, t)$ the equation of the displacement calculated through the modal superposition approach as

$$v(0, t) = \left. \frac{\partial u}{\partial t}(x, t) \right|_{x=0} = i\omega \cdot u(0, t) = i\omega \sum_i \frac{\Phi_i(0) \cdot \Phi_i(0)}{-\omega^2 m_{q_i} + (1 + i\eta) k_{q_i}} F_0 e^{i\omega t} \quad (3.4)$$

Driving-point impedance wave propagation solution

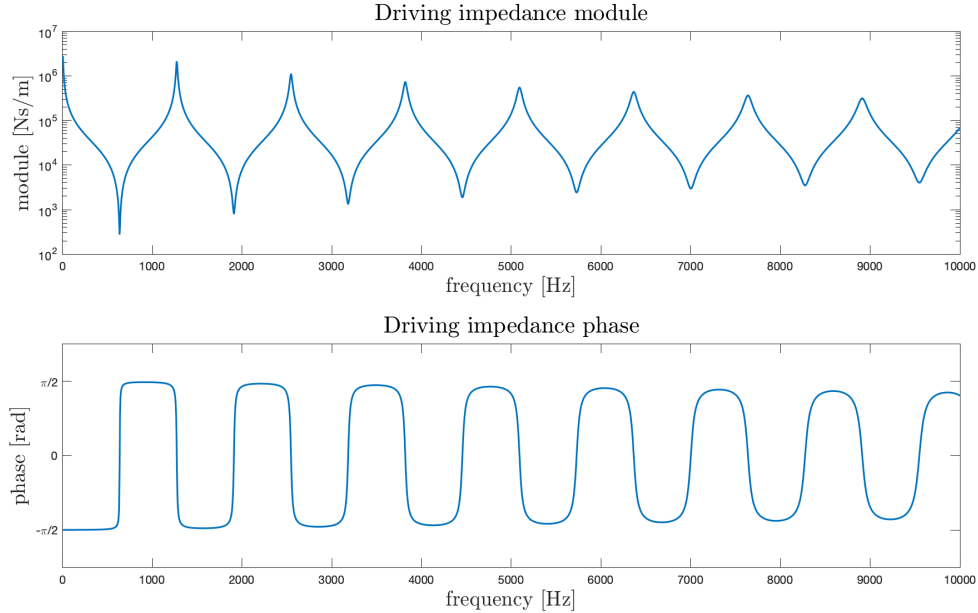


Figure 3.1: Driving-point impedance wave propagation solution

from this we can calculate the driving-point impedance as

$$Z(\omega) = \frac{F_0 e^{i\omega t}}{\left. \frac{\partial u}{\partial t}(x, t) \right|_{x=0}} = \frac{F_0 e^{i\omega t}}{i\omega \sum_i \frac{\Phi_i(0) \cdot \Phi_i(0)}{-\omega^2 m_{q_i} + (1+i\eta) k_{q_i}} F_0 e^{i\omega t}} = \frac{1}{i\omega \sum_i \frac{\Phi_i(0) \cdot \Phi_i(0)}{-\omega^2 m_{q_i} + (1+i\eta) k_{q_i}}} \quad (3.5)$$

In figure 3.2 the result for the driving-point impedance calculated considering 8 modeshapes corresponding to the range from 0 to 10 kHz is shown. The figure 3.3 is useful to show how the number of modeshapes considered for the *modal superposition approach* is useful to determine the precision of the impedance approximated to the one determined by the wave propagation solution. It is clearly noticeable how the use of only 8 modes ([0 – 10] kHz) allows to create the correct number of resonances, and to determine precisely the position of only those which are positioned in the low-frequency range. Whereas increasing the number of modes considered to 50 or 100 allows to approximate more and more precisely the behaviour determined by the wave propagation solution.

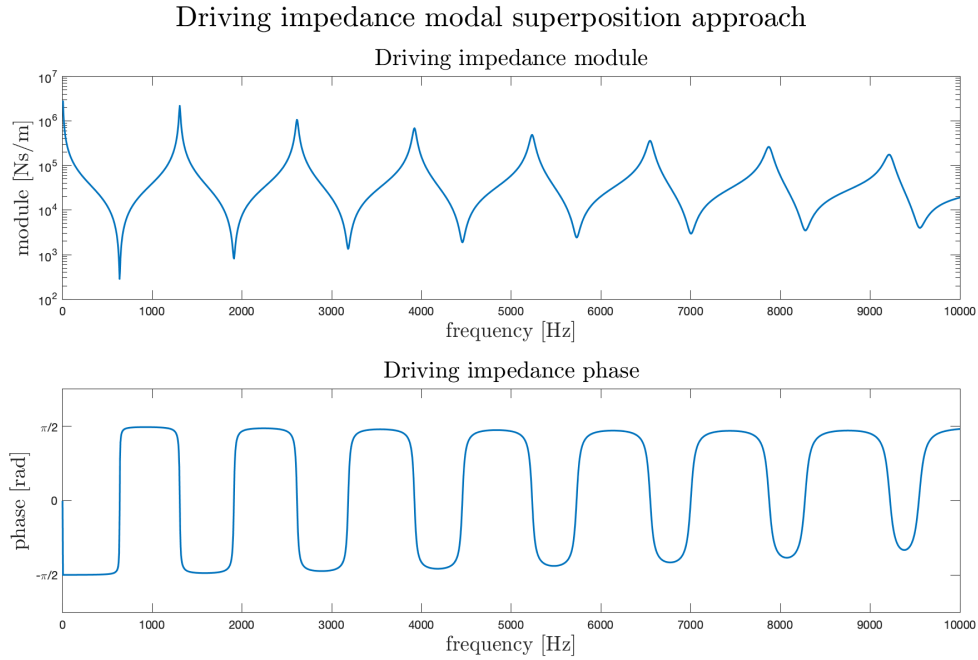


Figure 3.2: Driving-point impedance wave propagation solution

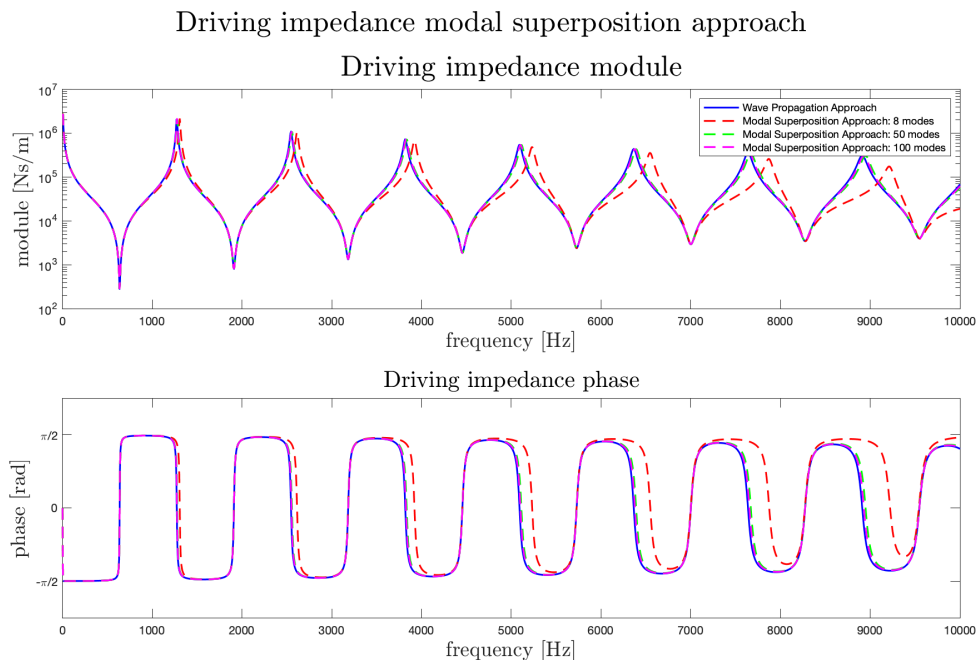


Figure 3.3: Driving-point impedance wave propagation solution

VIBRATION ANALYSIS AND VIBROACOUSTICS

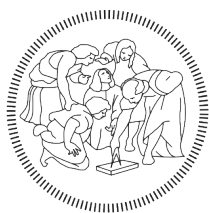
SECOND ASSIGNMENT

Report

Experimental Modal Analysis of a Violin

Students

Marco BERNASCONI - 10669941
Alberto DOIMO - 10865196



POLITECNICO
MILANO 1863

Contents

1	Introduction	2
2	Vibration Modes Identification	3
2.1	Modal Parameter Estimation	3
2.1.1	Residual Minimization Technique to reconstruct the Experimental FRF .	5
3	Mode Shapes Visualization	6
3.0.1	Comparison between experimental and reconstruncted FRFs	6
3.1	Visualization of the Mode Shape of ω_1	7
3.2	Visualization of the Mode Shape of ω_2	9
3.3	Visualization of the Mode Shape of ω_3	10
3.4	Visualization of the Mode Shape of ω_4	11

Chapter 1

Introduction

Different FRFs [$\frac{m}{Ns^2}$] have been obtained performing a hammer test on a violin through a roving hammer procedure. This procedure consists in moving only the hammer to different points on the violin while keeping the measurement point fixed. The excitement points are shown in Fig.1.1. The file *Data.mat* contains all the measured FRFs along with a frequency vector [0, 1000][Hz] that contains the frequencies at which the FRFs have been computed, the x and y coordinates for the excitement grid and the coordinates for the contour of both the front and back plate.

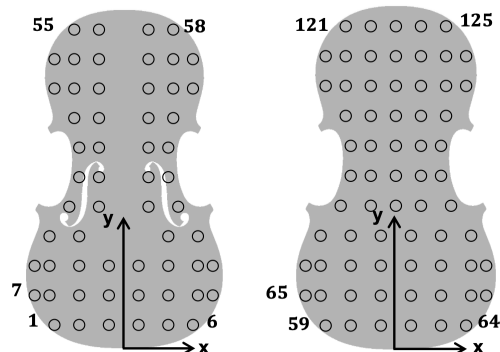


Figure 1.1: Excitement points. 1:58 are on the top plate while 59:125 are on the back plate

Chapter 2

Vibration Modes Identification

The Steady State amplitude of the i^{th} modeshape $q_{i,0}(t)$ when the system is subjected to a force $X_k^{(i)}F_k(t)$ which is imposed on the coordinate identified by the k^{th} index is:

$$q_{i,0} = \frac{X_k^{(i)}F_{k,0}}{-m_{q_i}\omega^2 + ic_{q_i}\omega + k_{q_i}} \quad (2.1)$$

where m_{q_i} , c_{q_i} and k_{q_i} are the mass, damping and stiffness of the i^{th} mode.

From the modal superposition theory it is possible to derive a formulation for the FRF of a system excited at a point k when the response is measured at point j :

$$G_{j,k} = \frac{X_{j,0}}{F_{k,0}} = \sum_i \frac{X_j^{(i)} \cdot X_k^{(i)}}{-m_{q_i}\omega^2 + ic_{q_i}\omega + k_{q_i}} = \sum_i \frac{X_j^{(i)} \cdot X_k^{(i)}/m_{q_i}}{-\omega^2 + 2i\omega_i\omega\xi_i + \omega_i^2} = \quad (2.2)$$

where ω_i are the resonant frequencies of the system and $\xi_i = \frac{c_{q_i}}{2m_{q_i}\omega_i}$ is the adimensional damping ratio.

2.1 Modal Parameter Estimation

The natural frequencies and the adimensional damping coefficients of the systems can be obtained by considering a subset of the frequencies of the FRF centered around one of the peaks of the function. By defining a $[\omega_{inf}, \omega_{sup}]$ range where $\omega_{inf} < \omega_i < \omega_{sup}$, and under the assumption that $\xi_i \ll 1$, we can assume that the position of the peak is ω_i . This is possible because with this assumption the system is lightly damped and the resonances are not shifted from the natural frequencies. The actual value of ξ_i will be evaluated from the phase of the FRF by the phase derivation method:

$$\xi_i = -\frac{1}{\omega_i \left. \frac{\partial \angle G_{j,k}(\omega)}{\partial \omega} \right|_{\omega_i}} \quad (2.3)$$

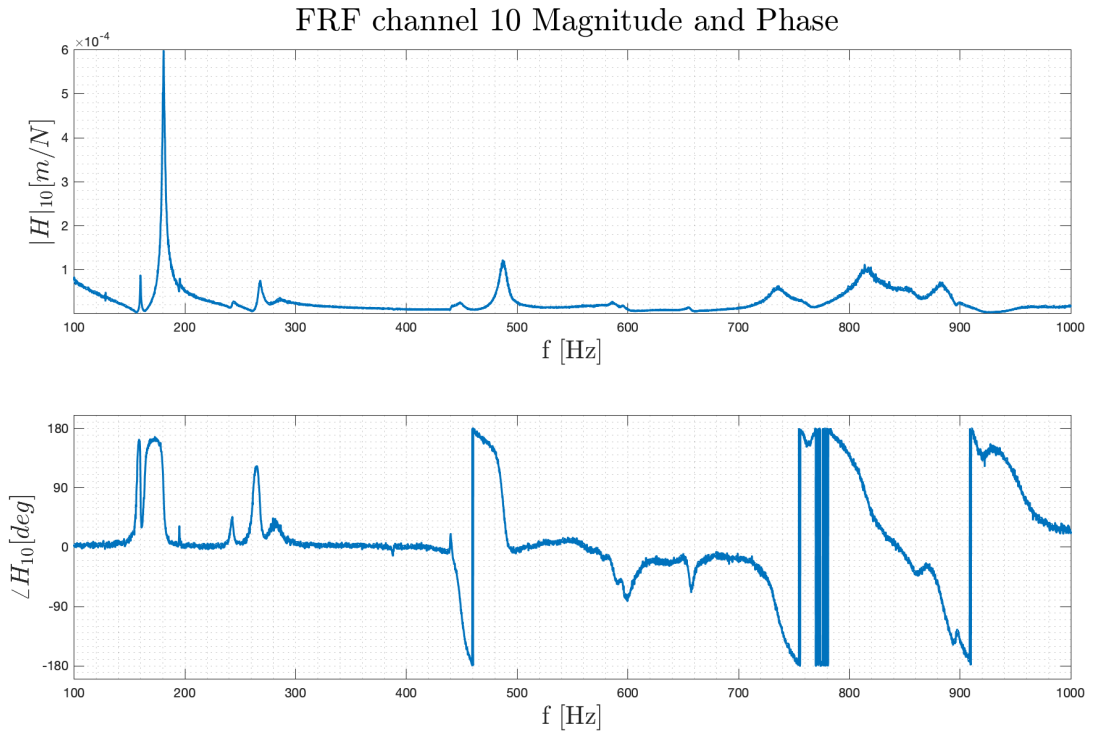


Figure 2.1: Front plate FRF at channel 10

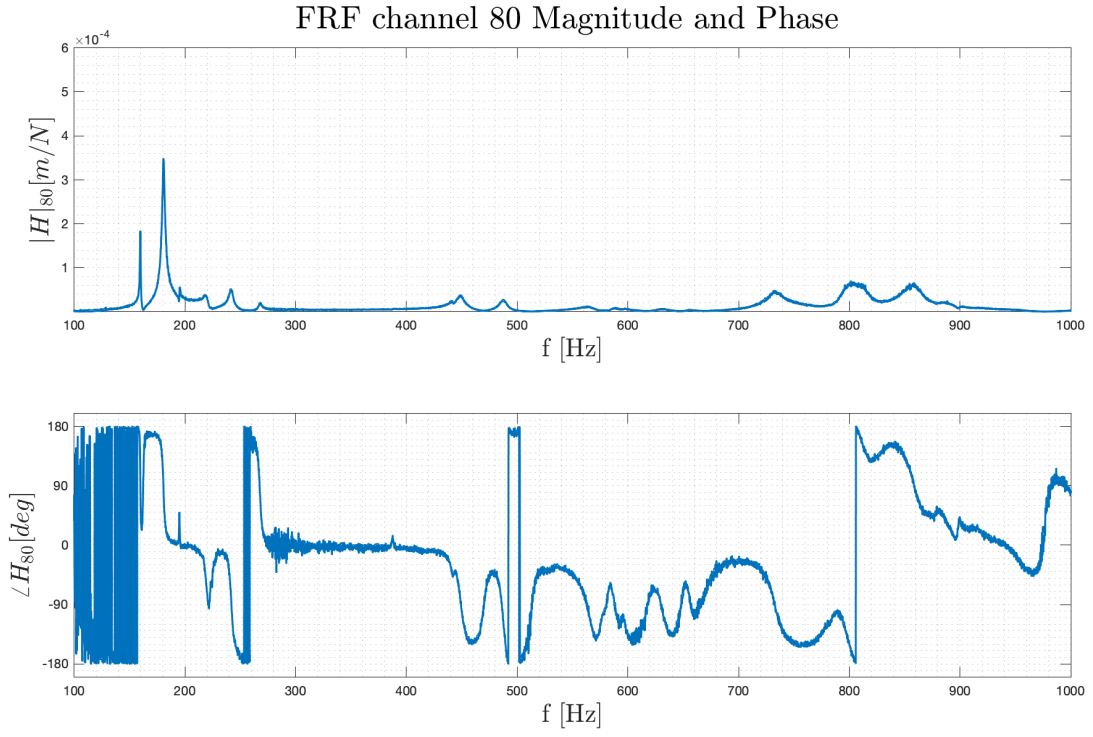


Figure 2.2: Front plate FRF at channel 10

In Fig.2.1 and 2.2 we see an example for the FRF taken from the front and the back plate. From these we can estimate the natural frequencies and the adimensional damping ratios for the four main modes which are shown in Tab.2.1

	ω	ξ
1	180.6	0.65
2	267.8	0.72
3	449	0.51
4	735.2	2.23

Table 2.1: Approximative values for ω and ξ for each mode

2.1.1 Residual Minimization Technique to reconstruct the Experimental FRF

Now we want to reconstruct the complete FRF of the violin in each channel by using the Residual Minimization Technique. This is done by approximating the contribution of the modeshapes to 3 different terms:

- A term to approximate the contribution of the mode in the range $[\omega_{inf}, \omega_{sup}]$
- A linear term $R_{j,k}^H$ to approximate the contribution of higher frequency modes in the quasi-static range $[\omega_{sup}, +\infty]$
- A decreasing term $R_{j,k}^L/\omega^2$ to approximate the contribution of the lower frequency modes in the seismographic range $[0, \omega_{inf}]$

The formula is:

$$G_{j,k}^{NUM}(\omega) = \frac{A_{j,k}^{(i)}}{-\omega^2 + i2\omega_i\xi_i\omega + \omega_i^2} + R_{j,k}^H + R_{j,k}^L/\omega^2 \quad (2.4)$$

Since the error function associated to the accuracy of the estimation depends non-linearly from the presented unknown parameters, an iterative minimization procedure is used. For this reason we use the MATLAB function `lsqnonlin()`.

Chapter 3

Mode Shapes Visualization

The visualization of the modes on the violin's plate will follow the same criteria used before: channel 10 and 80 are considered and both top and back plates are displayed. To obtain this graphical representation it is necessary to evaluate the amplitude of the estimated parameters A(i).

3.0.1 Comparison between experimental and reconstruncted FRFs

Using the formula in Eq.2.4 we can reconstrunct the FRF of a channel and compare it with the experimental FRF

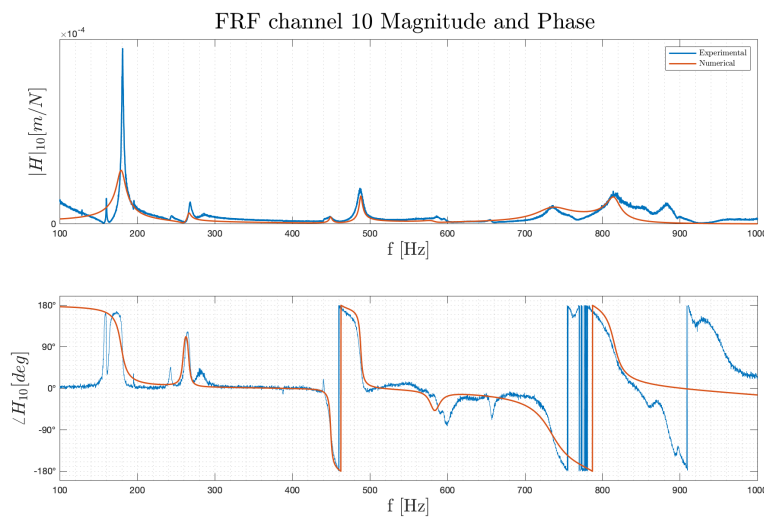


Figure 3.1: Magnitude and phase of the experimental and reconstruncted FRF at channel 10

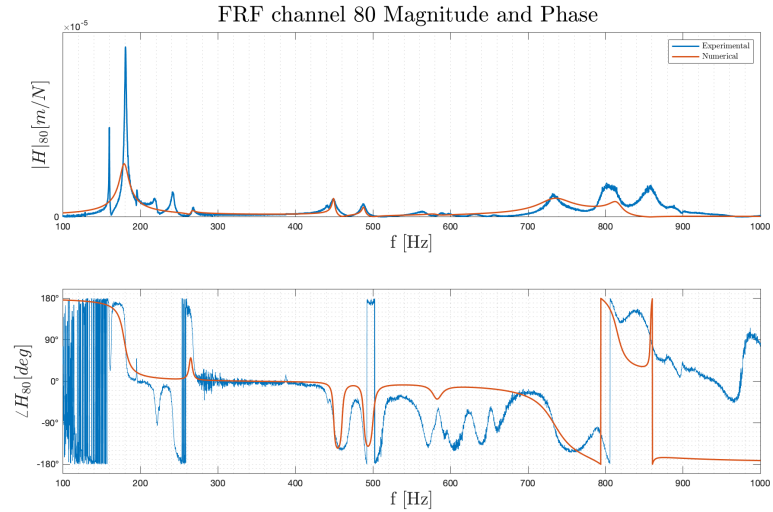


Figure 3.2: Magnitude and phase of the experimental and reconstructed FRF at channel 80

3.1 Visualization of the Mode Shape of ω_1

Channel 10:

$$f_i : 180.6\text{Hz}, h_i = 0.653$$

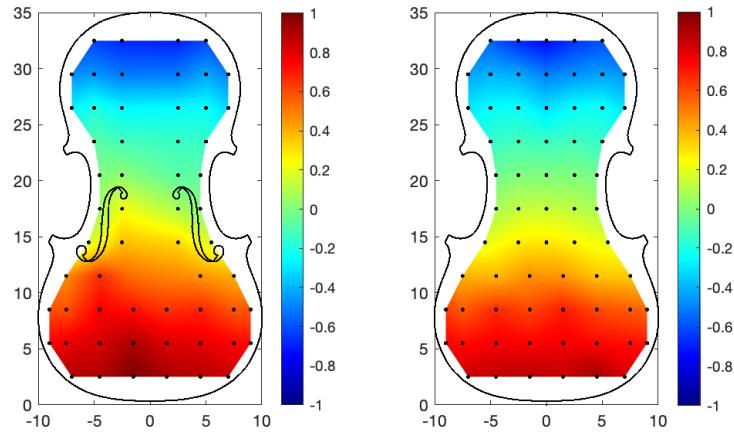


Figure 3.3: Left image: top plate. Right image: back plate

Channel 80:

$$f_i : 180.6\text{Hz}, h_i = 0.5752$$

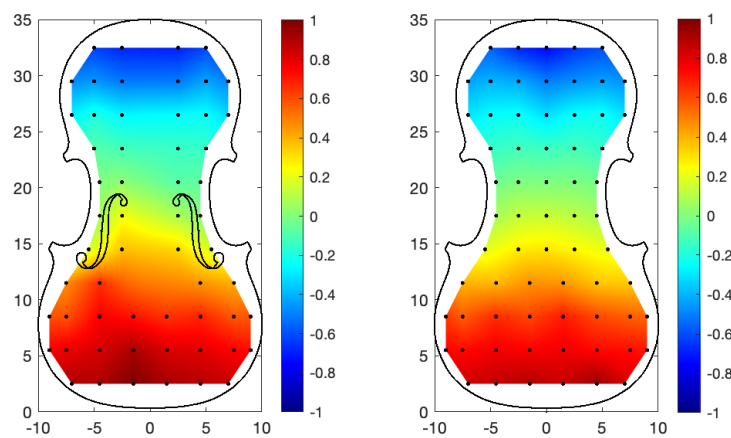


Figure 3.4: Left image: top plate. Right image: back plate

3.2 Visualization of the Mode Shape of ω_2

Channel 10:

$$f_i : 267.8 \text{Hz}, h_i = 0.72$$

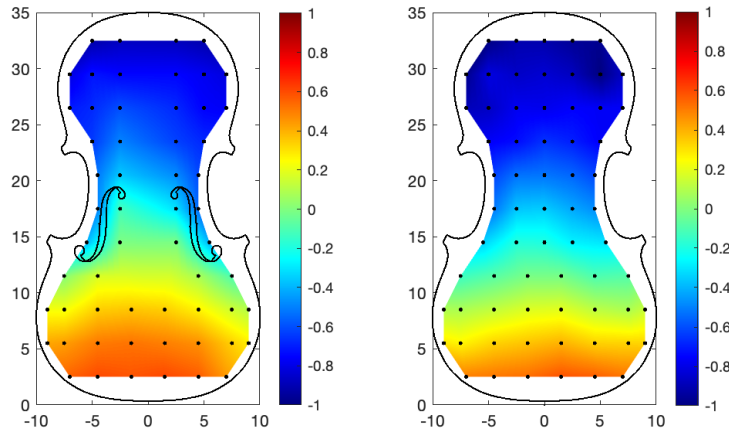


Figure 3.5: Left image: top plate. Right image: back plate

Channel 80:

$$f_i : 267.8 \text{Hz}, h_i = 0.9214$$

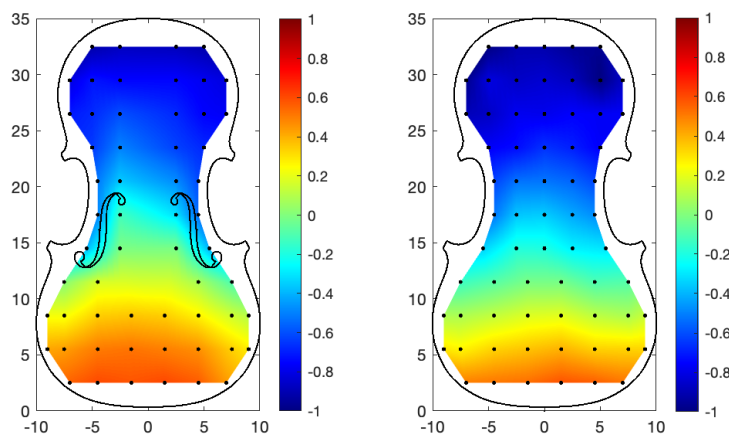


Figure 3.6: Left image: top plate. Right image: back plate

3.3 Visualization of the Mode Shape of ω_3

Channel 10:

$$f_i : 449Hz, h_i = 0.5144$$

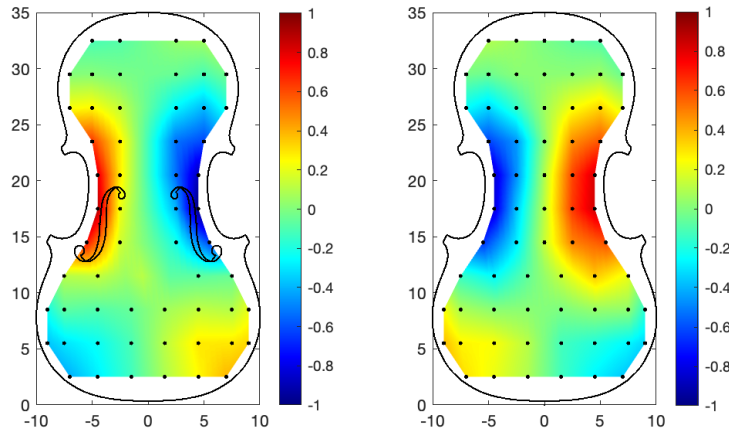


Figure 3.7: Left image: top plate. Right image: back plate

Channel 80:

$$f_i : 449Hz, h_i = 34.9953$$

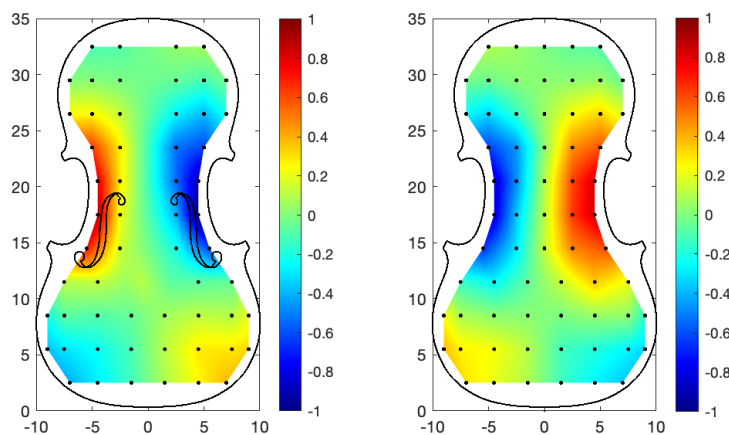


Figure 3.8: Left image: top plate. Right image: back plate

3.4 Visualization of the Mode Shape of ω_4

Channel 10:

$$f_i : 735.2\text{Hz}, h_i = 2.23$$

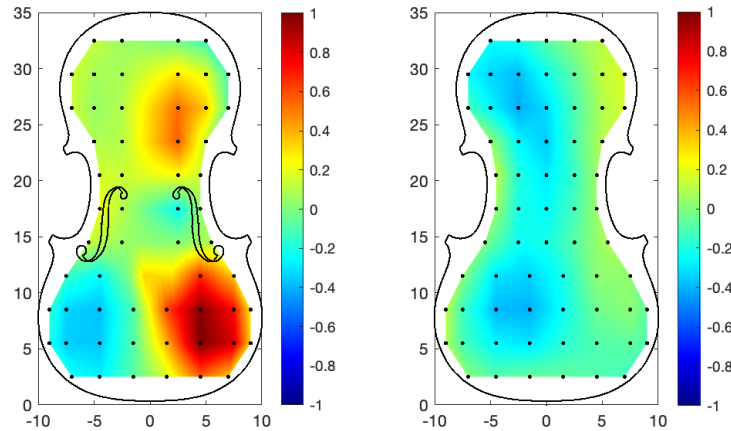


Figure 3.9: Left image: top plate. Right image: back plate

Channel 80:

$$f_i : 735.2\text{Hz}, h_i = 0.6228$$

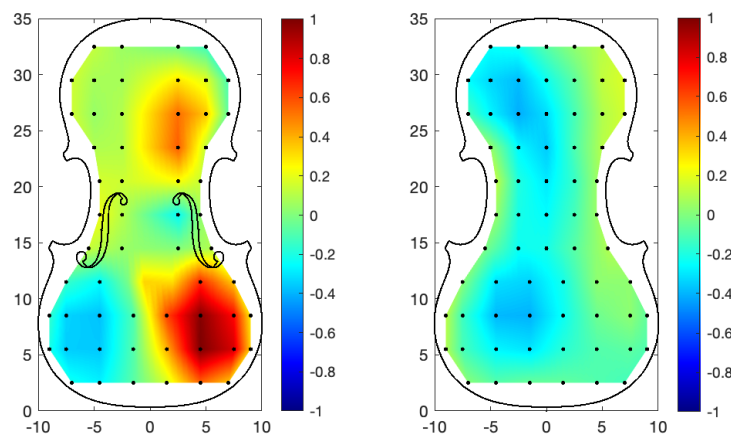


Figure 3.10: Left image: top plate. Right image: back plate